Ligand-induced distortion of a tetranuclear manganese butterfly complex

Rashmi Bagai, Khalil A. Abboud and George Christou*

Received 14th February 2006, Accepted 17th March 2006
First published as an Advance Article on the web 12th April 2006
DOI: 10.1039/b602192a

The reaction of the pentadentate Schiff-base ligand 1,3-bis(salicylideneamino)-2-propanol (salproH_3) with $[Mn_3O(O_2CR)_6(py)_3]$ (R = Me, Et, Bu^t) gives the corresponding tetranuclear manganese product $[Mn_4O_2(O_2CR)_5(salpro)]$ ($4Mn^{III}$). The syntheses, structure and magnetochemical characterization of these complexes are reported. The structure of the $[Mn_4(\mu_3\text{-}O)_2]^{8+}$ is butterfly-like much more closed than in previous complexes with this core as a result of the alkoxide oxygen of the salpro ligand bridging the two wingtip Mn atoms. Variable-temperature, solid-state magnetic susceptibility studies reveal that these complexes possess $S = 0$ ground state spins. Fitting of the magnetic susceptibility data to the theoretical $\chi_M T$ *vs.* T expression derived for a C_{2v} symmetry complex, assuming an isotropic Heisenberg spin-Hamiltonian and using the Van Vleck equation, revealed that the various exchange parameters are all antiferromagnetic, and the core thus experiences spin frustration effects.

Introduction

Manganese cluster chemistry has been receiving a great deal of attention for two main reasons: (i) the occurrence of this metal in a variety of manganese-containing biomolecules, the most important of which is the water oxidizing complex (WOC) in the photosynthetic apparatus of green plants and cyanobacteria. This contains an oxide-bridged Mn_4 unit and is responsible for essentially all the oxygen gas on this planet.[1] This has stimulated the search for tetranuclear Mn complexes with oxide bridges that can serve as models for the WOC.[2] (ii) High nuclearity Mn clusters often display large ground state spin (S) states as a result of ferromagnetic exchange interactions and/or spin frustration effects. If such molecules with large S values also possess significant magnetoanisotropy of the Ising (easy-axis) type, then they have the potential to be single-molecule magnets (SMMs).[3] These are individual molecules that possess a significant barrier (*vs.* kT) to magnetization relaxation and thus exhibit the ability to function as magnets below their blocking temperature (T_B).

Our group has had a strong interest over many years in the development of synthesis methodologies to oxide-bridged Mn clusters, primarily with carboxylate ligands. One synthetic strategy that has proven particularly useful has been the use of the preformed clusters of general formula $[Mn_3O(O_2CR)_6(L)_3]^{0,+}$ as starting materials in reactions with a variety of co-reagents.[4–6] A wide range of the latter have been employed, almost always bidentate or higher denticity chelates, and often ones that also contain potentially bridging alkoxide groups. Such reactions have often caused higher-nuclearity products to form, both homo- and mixed-valent. The present work represents an extension of this approach. As part of our continuing search for new preparative routes to high nuclearity Mn clusters, we have investigated the reactivity of the pentadentate Schiff-base ligand 1,3-bis(salicylideneamino)-2-propanol (salproH_3).

Department of Chemistry, University Of Florida, Gainesville, FL, 32611-7200, USA. E-mail: christou@chem.ufl.edu

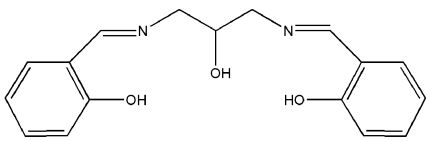

SalproH$_3$

This group has been used previously by others in Mn chemistry and had afforded mononuclear, dinuclear and polymeric complexes.[7] With this precedent, we believed that salproH_3 might prove a route to more new Mn compounds under appropriate reaction conditions, and decided to investigate its reactions with the $[Mn_3O(O_2CR)_6(L)_3]$ complexes. It was obvious that pentadentate salproH_3 cannot bind to these Mn_3 species without resulting in a serious structural perturbation, and a possible nuclearity change. Indeed, as will be described below, these reactions have yielded new types of Mn_4 complexes with a core structure that is distinctly different from those seen before. The syntheses, structures and magnetochemical properties of these complexes are the subject of this paper.

Experimental

Syntheses

All preparations were performed under aerobic conditions using reagents and solvents as received. The compound salproH_3 was synthesized using the reported procedure.[8] $[Mn_3O(O_2CMe)_6(py)_3]\cdot py$ (**1**), $[Mn_{12}O_{12}(O_2CMe)_{16}(H_2O)_4]$ (**2**), $[Mn_3O(O_2CEt)_6(py)_3]\cdot py$ (**3**), $[Mn_3O(O_2CBu^t)_6(py)_3]$ (**4**), were synthesized as reported elsewhere.[9,10]

$[Mn_4O_2(O_2CMe)_5(salpro)]$ (5).

Method A. To a stirred solution of salproH_3 (0.05 g, 0.17 mmol) in CH_2Cl_2–MeOH (3:2 mL) was added triethylamine (83 μL, 0.57 mmol) followed by the addition of a solution of complex **1** (0.22 g, 0.25 mmol) in CH_2Cl_2 (10 mL). This solution was left

under magnetic stirring for 30 min and then filtered through a medium frit. The brown filtrate was left undisturbed to evaporate slowly, giving X-ray quality crystals that grew slowly over five days. These were collected by filtration, washed with CH_2Cl_2 and dried *in vacuo.* Yield 56%. Anal. Calc. for **5**·CH_2Cl_2 ($C_{28}H_{32}Mn_4N_2O_{15}Cl_2$): C, 36.27; H, 3.48; N, 3.02. Found: C, 36.82; H, 3.64; N, 2.97%. IR (KBr, cm^{-1}): 3446br, 1625s, 1568s, 1445s, 1394s, 1297m, 1153m, 1092w, 1026m, 759m, 677s, 595s, 468m.

Method B. To a stirred solution of salproH$_3$ (0.20 g, 0.67 mmol) in MeCN–MeOH (3 : 2 v/v) was added triethylamine (83 μL, 0.57 mmol) followed by the addition of a solution of complex **2** (0.32 g, 0.17 mmol) in MeCN (10 mL). This solution was left under magnetic stirring for 1 h and then filtered through a medium frit. The homogeneous brown solution was left undisturbed for slow evaporation, giving X-ray quality crystals that grew slowly over the course of one week. These were collected by filtration, washed with acetonitrile, and dried *in vacuo.* Yield 16%. The product was identified as **5** by IR spectral comparison with material from Method A.

Method C. To a stirred solution of salproH$_3$ (0.05 g, 0.17 mmol) in MeCN–MeOH (3 : 2 v/v) was added triethylamine (83 μL, 0.57 mmol) followed by the addition of a solution of $Mn(O_2CMe)_3{\cdot}2H_2O$ (0.09 g, 0.34 mmol) in MeCN (10 mL). This solution was left under magnetic stirring for 30 min and then worked up as for Method B. Yield 28%. The product was identified as **5** by IR spectral comparison with material from Method A.

[$Mn_4O_2(O_2CEt)_5$(salpro)] (6). To a stirred solution of salproH$_3$ (0.05 g, 0.17 mmol) in CH_2Cl_2–MeOH (3 : 2 v/v) was added triethylamine (83 μL, 0.57 mmol) followed by the addition of a solution of complex **3** (0.31 g, 0.34 mmol) in CH_2Cl_2 (10 mL). This solution was left under magnetic stirring for 30 min and then filtered through a medium frit. X-Ray quality crystals were obtained over the course of three days by vapour-diffusing diethyl ether into the filtrate. The resulting crystals were collected by filtration, washed with ether, and dried *in vacuo.* Yield 22%. Anal. Calc. for **6**·CH_2Cl_2 ($C_{33}H_{42}Mn_4N_2O_{15}Cl_2$): C, 39.74; H, 4.24; N, 2.80. Found: C, 39.66; H, 4.21; N, 2.68%. IR (KBr, cm^{-1}): 3441br, 2879m, 1626s, 1572s, 1446m, 1404m, 1299m, 1150w, 1080w, 1031w, 750w, 676m, 598s, 467m.

[$Mn_4O_2(O_2CBu^t)_5$(salpro)] (7). To a stirred solution of salproH$_3$ (0.05 g, 0.17 mmol) in CH_2Cl_2–MeOH (3 : 2 v/v) was added triethylamine (83 μL, 0.57 mmol) followed by the addition of solution of complex **4** (0.29 g, 0.28 mmol) in CH_2Cl_2 (10 mL). This solution was left under magnetic stirring for 30 min and then filtered through a medium frit. X-Ray quality crystals were obtained during the course of five days by layering the filtrate with heptane and allowing the solvents to slowly mix. The resulting crystals were collected by filtration, washed with heptane and dried *in vacuo.* Yield 25%. Anal. Calc. for **7**·1/2CH_2Cl_2 ($C_{42.5}H_{61}Mn_4N_2O_{15}Cl$): C, 47.58; H, 5.83; N, 2.49. Found: C, 47.44; H, 5.86; N, 2.74%. IR (KBr, cm^{-1}): 3442br, 2959m, 1627m, 1560s, 1482m, 1447w, 1408m, 1358m, 1301m, 1221m, 1150w, 1029w, 895w, 757w, 678m, 599s, 439m.

X-Ray crystallography and solution of structure

Data were collected using a Siemens SMART PLATFORM equipped with a CCD area detector and a graphite monochromator utilizing Mo-Kα radiation ($\lambda = 0.71073$ Å). Suitable crystals of **5**·MeCN and **7**·MeOH·2CH_2Cl_2·C_7H_{16} were attached to glass fibres using silicone grease and transferred to a goniostat where they were cooled to 173 K for data collection. Cell parameters were refined using up to 8192 reflections. A full sphere of data (1850 frames) was collected using the ω-scan method (0.3° frame width). The first 50 frames were remeasured at the end of data collection to monitor the instrument and crystal stability (maximum correction on I was <1%). Absorption corrections by integration were applied based on measured indexed crystal faces.

The structures were solved by direct methods in *SHELXTL6*,[11] and refined using full-matrix least squares. The non-H atoms were treated anisotropically, whereas the hydrogen atoms were placed in ideal, calculated positions and refined as riding on their respective carbon atoms. In **5**·MeCN, the asymmetric unit consists of the Mn_4 cluster and a disordered MeCN molecule. A total of 465 parameters were refined in the final cycle of refinement using 5581 reflections with $I > 2\sigma(I)$ to yield R_1 and wR_2 of 4.13 and 8.28%, respectively. In **7**·MeOH·2CH_2Cl_2·C_7H_{16}, the asymmetric unit consists of the cluster and one heptane, one methanol, and two dichloromethane molecules. The three methyl groups on C17 are disordered, and each dichloromethane molecule has one chlorine atom disordered. In each case, two disorder sites were included, and their site occupation factors independently refined. A total of 723 parameters were included in the final cycle of refinement using 9336 reflections with $I > 2\sigma(I)$ to yield R_1 and wR_2 of 4.73 and 12.20%, respectively. Refinement was done using F^2.

CCDC reference numbers 298092 and 298093 for **5**·MeCN and **7**·MeCN·2CH_2Cl_2·C_7H_{16} respectively.

For crystallographic data in CIF or other electronic format see DOI: 10.1039/b602192a

Other studies

Elemental analyses (C, H and N) were performed by the in-house facilities of the Chemistry Department, University Of Florida. Infrared spectra (KBr) were recorded from 400 to 4000 cm^{-1} using a Nicolet Nexus 670 FT-IR spectrophotometer. Variable-temperature dc magnetic susceptibility data down to 5.0 K were collected at the University of Florida using a Quantum Design MPMS-XL SQUID magnetometer equipped with a 7 Tesla magnet. Pascal's constants were used to estimate diamagnetic corrections, which were subtracted from the experimental susceptibility to give the molar paramagnetic susceptibility. Powdered crystalline samples were embedded in eicosane to prevent torquing.

Results and discussion

Syntheses

Trinuclear $[Mn_3O(O_2CR)_6(L)_3]^{0,+}$ clusters have proven to be very useful starting materials for the synthesis of higher nuclearity products, affording complexes of nuclearity 4–18. For example, reaction of $[Mn_3O(O_2CMe)_6(py)_3]^+$ with 2,2′ bipyridine (bpy)[4] or picolinate (pic^-)[5] gave $[Mn_4O_2(O_2CMe)_7(bpy)_2]^+$ and $[Mn_4O_2(O_2CMe)_7(pic)_2]^-$ salts, respectively. In addition, the reaction of a mixture of $[Mn_3O(O_2CMe)_6(py)_3]^+$ and $[Mn_3O(O_2CMe)_6(py)_3]{\cdot}py$ with 2-(hydroxyethyl)pyridine (hepH) gave $[Mn_{18}O_{14}(O_2CMe)_{18}(hep)_4(hepH)_2(H_2O)_2]^{2+}$.[6] However, a chelating

reagent is not always necessary: Treatment of $[Mn_3O(O_2CPh)_6(py)_2(H_2O)]$ with phenol gives $[Mn_6O_2(O_2CPh)_{10}(py)_2(MeCN)_2]$, the phenol merely acting as a reducing agent and triggering dimerization.[12] Thus, the choice of chelating or other co-reagent and the reaction conditions have significant effect not only on the nuclearity of the product but also on its metal topology.

Along the same lines, the reaction of $[Mn_3O(O_2CMe)_6(py)_3]\cdot py$ with salproH$_3$ and NEt$_3$ in a roughly 3 : 2 : 6 molar ratio in CH_2Cl_2–MeOH gave the novel tetranuclear complex $[Mn_4O_2(O_2CMe)_5(salpro)]$ (**5**). Its formation can be summarized in eqn (1).

$$2\,[Mn_3O(O_2CMe)_6(py)_3] + salproH_3 \rightarrow [Mn_4O_2(O_2CMe)_5(salpro)] + 7\,MeCO_2^- + 2\,Mn^{2+} + 6\,py + 3\,H^+ \quad (1)$$

The reaction is sensitive to the Mn_3:salproH$_3$ ratio, and complex **5** is obtained only when 0.5–0.7 equivalents of salproH$_3$ per Mn_3 is employed. We also found that the mixed CH_2Cl_2–MeOH solvent system is very important; no reaction was observed when the reaction was performed in CH_2Cl_2 alone, and only starting material was recovered. Presumably, the more polar MeOH facilitates the necessary proton transfer steps. However, the yield of the product decreases as the concentration of MeOH increases beyond that described in the Experimental section, presumably due to the solubility of the product. Thus, a controlled amount of MeOH is essential for a high yield reaction. However, the same product was obtained using a CH_2Cl_2–EtOH solvent system. Further investigation showed that the same complex **5** was also obtained from MeCN–MeOH. Also the same product is obtained in the absence of base but in lower yield.

Since complex **5** was obtained from a trinuclear starting material, we wondered if the same product would also result if we employed a higher nuclearity reagent, and thus explored the reaction of salproH$_3$ with $[Mn_{12}O_{12}(O_2CMe)_{16}(H_2O)_4]$, which contains 8 Mn(III) and 4 Mn(IV). Thus, an MeCN–MeOH solution of $[Mn_{12}O_{12}(O_2CMe)_{16}(H_2O)_4]$ was treated with 4 equivalents of salproH$_3$, and the same product, complex **5**, was indeed again obtained, but only in poor yield (16%). The filtrate was still intensely colored, but we did not pursue additional products of this reaction.

We also obtained complex **5** when the $[Mn_3O(O_2CMe)_6(py)_3]\cdot py$ starting material was replaced with "$Mn(O_2CMe)_3\cdot 2H_2O$". This "manganese(III) acetate" is really a polymer of Mn_3 trinuclear units similar to those in $[Mn_3O(O_2CMe)_6(py)_3]\cdot py$, and so it was perhaps not surprising that its reaction with salproH$_3$ gave the same product.

Access to other carboxylate derivatives of **5** is possible using the described procedure of Method A. Thus, the reaction using the R = Et (propionate) or Bu^t (pivalate) derivatives of $[Mn_3O(O_2CR)_6(py)_3]$ gave the corresponding $[Mn_4O_2(O_2CR)_5(salpro)]$ complexes **6** and **7**, respectively. This provides access to more soluble versions of this new structural type of Mn_4 complex.

Structural description of $[Mn_4O_2(O_2CMe)_5(salpro)]\cdot MeCN$ and $[Mn_4O_2(O_2CBu^t)_5(salpro)]\cdot MeOH\cdot 2CH_2Cl_2\cdot C_7H_{16}$

The crystallographic data and structure refinement details for **5**·MeCN and **7**·MeOH·2CH$_2$Cl$_2$·C$_7$H$_{16}$ are listed in Table 1. The structures of **5** and **7** are shown in Fig. 1, and selected interatomic distances and angles for **5** are listed in Table 2.

Table 1 Crystallographic data for **5**·MeCN and **7**·MeOH·2CH$_2$Cl$_2$·C$_7$H$_{16}$

Empirical formula	$C_{29}H_{33}Mn_4N_3O_{15}$	$C_{52}H_{84}Cl_4Mn_4N_2O_{16}$
M	883.34	1354.77
Space group	$P2_1/n$	$P2_1/n$
a/Å	9.3368(6)	17.7518(13)
b/Å	22.5058(15)	17.3654(12)
c/Å	16.5079(11)	21.4029(15)
β/°	90.954(1)	100.856(1)
V/Å^3	3468.4(4)	6479.7(8)
Z	4	4
D_c/g cm^{-3}	1.692	1.389
T/K	173(2)	173(2)
λ(Mo-Kα)/Å	0.71073	0.71073
μ(Mo-Kα)/cm^{-1}	1.497	0.988
R_1 (wR_2)[a,b]	0.0413 (0.0828)	0.0473 (0.1220)

[a] $R_1 = \sum\|F_o\| - \|F_c\|/\sum\|F_o\|$. [b] $wR_2 = [\sum[w(F_o^2 - F_c^2)^2]/\sum[(wF_o^2)^2]]^{1/2}$, where $w = 1/[\sigma^2(F_o^2) + (mp)^2 + np]$, $p = [\max(F_o^2,0) + 2F_c^2]/3$, m and n are constants.

Table 2 Selected interatomic distances (Å) and angles (°) for **5**·MeCN

Mn1–O3	1.8859(19)	Mn3–O2	1.8884(19)
Mn1–O2	1.8906(18)	Mn3–O3	1.9062(18)
Mn1–O4	1.946(2)	Mn3–O12	1.9452(19)
Mn1–O6	1.956(2)	Mn3–O10	1.950(2)
Mn1–O5	2.0768(19)	Mn3–O11	2.085(2)
Mn2–O8	1.864(2)	Mn4–O14	1.8768(19)
Mn2–O2	1.9090(18)	Mn4–O3	1.9145(18)
Mn2–N1	1.972(2)	Mn4–N2	1.972(2)
Mn2–O1	1.9905(18)	Mn4–O1	1.9776(18)
Mn2–O7	2.206(2)	Mn4–O15	2.222(2)
Mn2–O9	2.238(2)	Mn4–O13	2.271(2)
Mn1···Mn2	3.1713(6)	Mn2···Mn3	3.1763(6)
Mn1···Mn3	2.7704(6)	Mn3···Mn4	3.1803(6)
Mn1···Mn4	3.1959(6)		
Mn1–O2–Mn3	94.30(8)	Mn4–O3–Mn3	112.69(9)
Mn1–O3–Mn4	114.47(9)	Mn2–O1–Mn4	133.88(9)
Mn2–O2–Mn1	113.16(9)	Mn1–O3–Mn3	93.87(8)
Mn2–O2–Mn3	113.53(9)	O2–Mn3–O12	170.65(8)
O3–Mn1–O4	168.79(9)	O3–Mn3–O10	165.26(8)
O2–Mn1–O6	167.88(8)	O3–Mn4–N2	174.03(9)
O2–Mn2–N1	176.64(9)	O14–Mn4–O1	172.54(8)
O8–Mn2–O1	172.88(9)		

Complex **5** crystallizes in monoclinic space group $P2_1/n$. It contains a $[Mn_4O_2]^{8+}$ core with peripheral ligation provided by five doubly-bridging acetate groups and one pentadentate salpro^{3-} ligand (Fig. 1, top). The core can be described as derived from two triangular, oxide-bridged $[Mn_3O]$ units sharing an edge and thus giving a $[Mn_4O_2]$ butterfly-like core as found in several other Mn_4 complexes (as well as with other transition metals), for example, $[Mn_4O_2(O_2CMe)_7(bpy)_2](ClO_4)$.[4] Atoms Mn(1) and Mn(3) occupy the 'body' positions of the butterfly and are five-coordinate (square pyramidal), and Mn(2) and Mn(4) occupy the 'wingtip' positions and are six-coordinate (octahedral). However, the $[Mn_4O_2]$ in **5** is much more closed up, *i.e.* a more acute V-shape, than normally found in such butterfly units (Fig. 2). This is reflected in the dihedral angle between the two Mn_3 planes, which is 79.2° in **5** compared with 135° in $[Mn_4O_2(O_2CMe)_7(bpy)_2](ClO_4)$,[4] which is typical of previous butterfly complexes. This can clearly be assigned to the fact that the wingtip Mn atoms of the butterfly

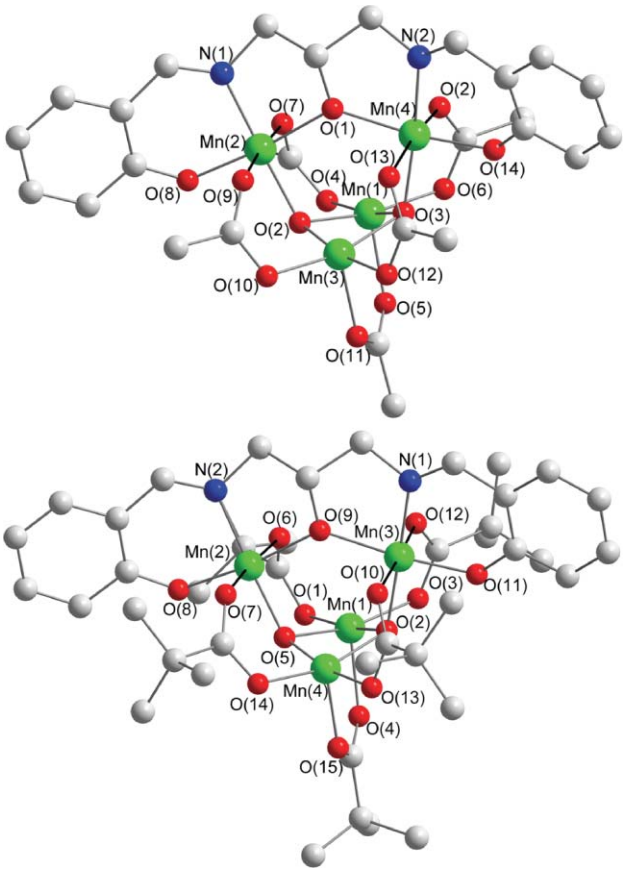

Fig. 1 Labeled structure of **5** (top) and **7** (bottom). Hydrogen atoms have been omitted for clarity. Jahn–Teller axes on Mn(III) are shown in black.

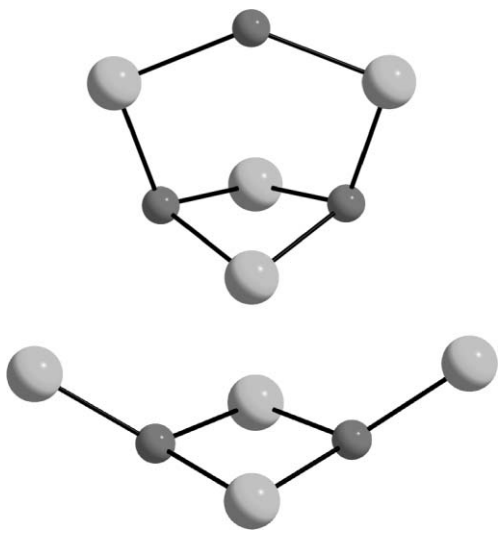

Fig. 2 Comparison of the cores of **5** and **7** (top) with that of the normal butterfly complexes (bottom).

topology, Mn(2) and Mn(4), are mono-atomically bridged by the salpro^{3-} O atom O(1) (Fig. 2, top). In fact, this drastic closing up of the butterfly makes the core of **5** intermediate between a butterfly and a cubane (*i.e.* tetrahedral) Mn_4 topology. There is a

Table 3 Bond valence sums[a] for manganese atoms of complex **5**

	Mn(II)	Mn(III)	Mn(IV)
Mn1	3.0738	*2.8116*	2.9517
Mn2	3.2858	*3.0437*	3.1333
Mn3	3.0412	*2.7817*	2.9204
Mn4	3.2343	*3.1639*	3.0820

[a] The italicized value is the one closest to the actual charge for which it was calculated. The oxidation state of a particular atom can be taken as the nearest whole number to the underlined value.

carboxylate group bridging each body–wingtip Mn pair, and a fifth carboxylate bridges the body–body Mn pair. The pentadentate salpro^{3-} ligand completes the peripheral ligation, chelating each wingtip Mn atom and bridging them *via* O(1).

All the Mn atoms are in the +3 oxidation state. This was established by qualitative consideration of the bond distances at each Mn, and confirmed quantitatively by bond valence sum (BVS) calculations (Table 3).[13] This also agreed with charge considerations and the overall neutrality of the molecule, as well as the clear presence of a Jahn–Teller (JT) distortion at near-octahedral Mn(2) and Mn(4) (Table 2), the JT axes being along the O(9),O(7) and O(2),O(13) vectors, respectively.

Complex **7** crystallizes in monoclinic space group $P2_1/n$. Selected interatomic distances and angles are listed in Table 4. Complex **7** is isostructural with complex **5** except for the difference in the carboxylate R groups. In particular, the dihedral angle between the two Mn_3 planes is 79.8°, and the Mn(III) JT axes have the same relative orientation. The bulky Bu^t groups thus have only a minimal effect on the structure, as expected from the lack of any steric interactions.

As discussed above, the structures of **5–7** can be considered closed-up versions of the familiar butterfly structures observed on several previous occasions in Mn(III) chemistry. It is thus of interest to structurally compare the two types, and this is done in Table 5. The metric parameters are fairly similar, as expected given that they are all Mn(III) species, but some overall conclusions can nevertheless be drawn. The closing up of the core of **5** and **7**, which is effectively a pivoting of the wingtip Mn atoms (Mn_w) about the μ_3-O^{2-} ions, has the effect of greatly decreasing the Mn_w–O–Mn_b as expected (by ~10–15°), but also slightly decreasing the Mn_b–O–Mn_b angles (by ~1–2°) as the central $[Mn_2O_2]$ rhombus buckles into a non-planar conformation. These angle changes are also reflected in the Mn ··· Mn separations, which all decrease by ~0.1–0.2 Å, except for the Mn_w ··· Mn_w separation which is much shorter in **5** and **7**.

Table 4 Selected interatomic distances (Å) and angles (°) for **7**·MeOH·$2CH_2Cl_2$·C_7H_{16}

Mn1–O5	1.910(2)	Mn4–O2	1.904(2)
Mn1–O2	1.887(2)	Mn2–O5	1.907(2)
Mn4–O5	1.888(2)	Mn3–O2	1.909(19)
Mn2–O9	1.984(2)	Mn3–O9	1.970(2)
Mn1–O5–Mn4	94.74(9)	Mn3–O2–Mn1	113.17(10)
Mn1–O2–Mn4	94.97(9)	Mn3–O2–Mn4	110.64(9)
Mn2–O5–Mn4	114.58(10)	Mn2–O9–Mn3	134.10(10)
Mn2–O5–Mn1	111.16(10)		

Table 5 Comparison of core parameters of selected $[Mn_4O_2]^{8+}$ butterfly complexes (Å, °)

Complex	$Mn_b \cdots Mn_b$	$Mn_b \cdots Mn_w$	$Mn_w \cdots Mn_w$	Mn_b–O	Mn_w–O	Mn_b–O–Mn_b	Mn_b–O–Mn_w	Mn_w–O–Mn_w	ref
5	2.770	3.171–3.196	3.651	1.886–1.906	1.909, 1.914,[a] 1.977, 1.991	94.30,93.87	112.7–114.5	133.88	[b]
7	2.794	3.136–3.193	3.640	1.887–1.910	1.907, 1.910,[a] 1.970, 1.984	94.97,94.74	110.6–114.6	134.1	[b]
$[Mn_4O_2(O_2CMe)_7(bpy)_2]^+$	2.848	3.299–3.385	5.593	1.889–1.930	1.804, 1.844	95.7,96.8	123.3–131.3	—	4
$[Mn_4O_2(O_2CMe)_7(pic)_2]^-$	2.842	3.308–3.406	—	1.888–1.910	1.840, 1.847	96.9	123.2–129.7	—	5
$[Mn_4O_2(O_2CEt)_7(bpya)_2]^+$	2.871	3.307–3.344	—	1.873–1.957	1.833, 1.838	97.07, 97.25	125.3–131.4	—	16

[a] Top and bottom entries refer to distances to oxide and alkoxide O atoms, respectively. [b] This work.

Magnetochemistry

Variable-temperature dc magnetic susceptibility data were collected in the 5.0–300 K range in a 1 kG (0.1 T) magnetic field on powdered microcrystalline samples of **5**·CH_2Cl_2, **6**·CH_2Cl_2 and **7**·1/2CH_2Cl_2 restrained in eicosane to prevent torquing, and the data are plotted as $\chi_M T$ *vs.* T in Fig. 3. For **5**·CH_2Cl_2, $\chi_M T$ smoothly decreases from 9.1 cm^3 K mol^{-1} at 300 K to 0.4 cm^3 K mol^{-1} at 5.0 K. The 300 K value is much less than the spin-only value of 12.0 cm^3 K mol^{-1} ($g = 2.0$) expected for four Mn(III) ions with non-interacting metal centers, indicating the presence of appreciable intramolecular antiferromagnetic interactions between the Mn ions, with the low-temperature data suggesting a spin $S = 0$ ground state.

Similar data were obtained for **6**·CH_2Cl_2 and **7**·1/2CH_2Cl_2, consistent with their isostructural nature and a minimal influence of the different ligands in the three complexes (Fig. 3).

The isotropic Heisenberg–Dirac–Van Vleck (HDVV) spin-Hamiltonian describing the exchange interactions within these Mn_4 complexes with virtual C_{2v} symmetry is given by eqn (2),

$$H = -2J_{bb}\hat{S}_1\cdot\hat{S}_3 - 2J_{bw}(\hat{S}_1\cdot\hat{S}_2 + \hat{S}_1\cdot\hat{S}_4 + \hat{S}_2\cdot\hat{S}_3 + \hat{S}_3\cdot\hat{S}_4) - 2J_{ww}\hat{S}_2\cdot\hat{S}_4 \quad (2)$$

where b = body, w = wingtip, $\hat{S}_i$ (i = 1–4) is the spin operator for metal atom Mn_i, and J is the exchange parameter. The exchange and atom labelling are summarized in the Scheme 1.

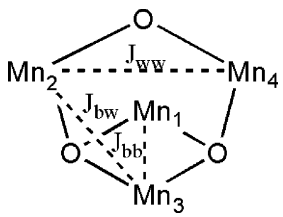

Scheme 1

The eigenvalues of the spin-Hamiltonian of eqn (2) can be determined analytically using the Kambe vector coupling method,[14] as described elsewhere for the more common butterfly complexes such as $[Mn_4O_2(O_2CMe)_7(bpy)_2]^+$, which also have C_{2v} symmetry.[4] Thus, use of the coupling scheme $\hat{S}_A = \hat{S}_1 + \hat{S}_3$, $\hat{S}_B = \hat{S}_2 + \hat{S}_4$, and $\hat{S}_T = \hat{S}_A + \hat{S}_B$ allows the spin-Hamiltonian to be transformed into the equivalent form given by eqn (3), where S_T is the total spin of the molecule.

$$H = -J_{bb}(\hat{S}_A{}^2 - \hat{S}_1{}^2 - \hat{S}_3{}^2) - J_{bw}(\hat{S}_T{}^2 - \hat{S}_A{}^2 - \hat{S}_B{}^2) - J_{ww}(\hat{S}_B{}^2 - \hat{S}_2{}^2 - \hat{S}_4{}^2) \quad (3)$$

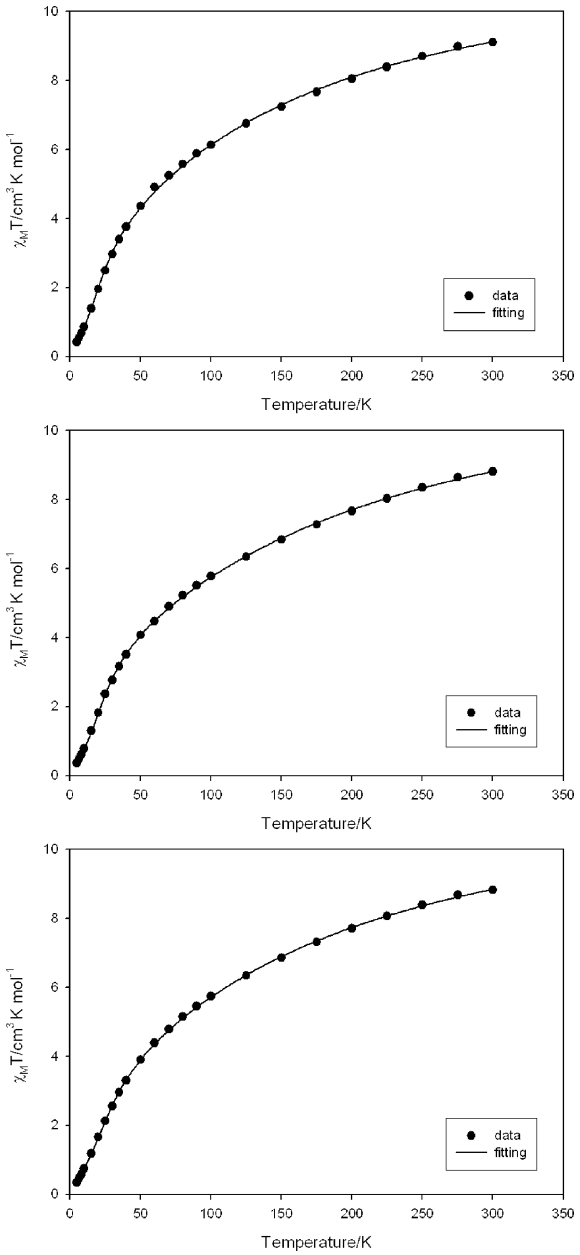

Fig. 3 $\chi_M T$ *vs.* T plots for **5**·CH_2Cl_2 (top), **6**·CH_2Cl_2 (middle) and **7**·1/2CH_2Cl_2 (bottom).

The eigenvalues of eqn (3) can be determined using the relationship $\hat{S}_i^2\psi = S_i(S_i + 1)\psi$, and are given in eqn (4), where

$$E|S_T, S_A, S_B\rangle = -J_{bb}[S_A(S_A + 1)] - J_{bw}[S_T(S_T + 1) - S_A(S_A + 1) - S_B(S_B + 1)] - J_{ww}[S_B(S_B + 1)] \quad (4)$$

$E|S_T, S_A, S_B\rangle$ is the energy of state $|S_T, S_A, S_B\rangle$, and constant terms contributing equally to all states have been omitted. The overall multiplicity of the spin system is 625, made up of 85 individual spin states ranging from $S_T = 0$–8.

An expression for the molar paramagnetic susceptibility, χ_M, was derived using the above and the Van Vleck equation,[15] and assuming an isotropic g tensor. This equation was then used to fit the experimental $\chi_M T$ *vs.* T data in Fig. 3 as a function of the three exchange parameters J_{bb}, J_{bw} and J_{ww} and the g factor. A contribution from temperature independent paramagnetism (TIP) was held constant at 400×10^{-6} cm^3 mol^{-1}. The obtained fits are shown as the solid lines in Fig. 3. The fitting parameters were: For **5**, $J_{bb} = -6.37$ cm^{-1}, $J_{bw} = -5.72$ cm^{-1}, $J_{ww} = -1.78$ cm^{-1} and $g = 2.00$; for **6**, $J_{bb} = -7.64$ cm^{-1}, $J_{bw} = -6.73$ cm^{-1}, $J_{ww} = -2.49$ cm^{-1} and $g = 2.00$; and for **7**, $J_{bb} = -7.37$ cm^{-1}, $J_{bw} = -6.57$ cm^{-1}, $J_{ww} = -1.79$ cm^{-1} and $g = 1.99$. The obtained values indicate that the ground state of the molecules is $|S_T, S_A, S_B\rangle = |0, 4, 4\rangle$, as anticipated from the low-temperature data in Fig. 3.

The exchange interactions within the Mn_4 cores of **5–7** are thus all antiferromagnetic and weak. The weakest is the J_{ww} between the wingtip Mn^{III} ions, but note that this is nevertheless a significant interaction relative to the others, unlike the more common types of butterfly species where this J_{ww} interaction is not a major contributor since the wingtip Mn atoms are not directly (monoatomically) bridged. Since the wingtip Mn atoms are bridged by an alkoxide O atom whereas the other Mn pairs are all bridged by either one or two oxide O atoms, it is qualitatively reasonable for J_{ww} to be the weakest interaction in the molecule, although the precise values of all the J parameters are the net sum of contributions from ferro- and antiferromagnetic pathways and thus it is difficult to rationalize their differences precisely.

It is, however, of interest to compare the exchange parameters for **5–7** with those for the more common type of Mn(III) butterfly complexes and see if any observed differences can be correlated with the structural differences mentioned earlier. In Table 6 are compared the exchange parameters for **5–7** with those for $[Mn_4O_2(O_2CMe)_7(bpy)_2]^+$ (**8**)[4], $[Mn_4O_2(O_2CMe)_7(pic)_2]^-$ (**9**)[5] and $[Mn_4O_2(O_2CEt)_7(bpya)_2]^+$ (**10**).[16] Although the J_{bw} interaction in **5–7** is within the range found for the previous complexes, the J_{bb} interaction in the former is distinctly weaker than in the latter. This is consistent with the significantly more acute angles at the μ_3-O^{2-} ions, since these will presumably weaken the antiferromagnetic contributions to the J_{bb} interaction by weakening the Mn(d_π)–O(p_π)–Mn(d_π) overlap that would be stronger when mediated by an essentially trigonal planar O atom as in **8–10**. The buckling of the central $[Mn_2O_2]$ no doubt also contributes to the change in J_{bb} by affecting the orbital overlap.

Table 6 Comparison of exchange parameters in $[Mn_4O_2]^{8+}$ complexes

Complex	J_{bb}[a]	J_{bw}[a]	J_{ww}[a]	g	ref
$[Mn_4O_2(O_2CMe)_5(salpro)]$	−6.37	−5.72	−1.78	2.00	[b]
$[Mn_4O_2(O_2CEt)_5(salpro)]$	−7.64	−6.73	−2.49	2.00	[b]
$[Mn_4O_2(O_2CBu^t)_5(salpro)]$	−7.37	−6.57	−1.79	1.99	[b]
$[Mn_4O_2(O_2CMe)_7(bpy)_2]^+$	−23.5	−7.8	—	2.0	4
$[Mn_4O_2(O_2CMe)_7(pic)_2]$	−24.6	−5.3	—	1.96	5
$[Mn_4O_2(O_2CEt)_7(bpya)_2]^+$	−25.7	−3.3	−0.77	1.99	16

[a] cm^{-1}. [b] This work.

The fact that $J_{bw} \approx J_{bb}$ in **5–7** is expected to have a clear impact on the ground state because the butterfly $[Mn_4O_2]^{8+}$ core in **8–10** has been well established from previous work to experience spin frustration effects as a result of the presence of triangular Mn_3 within its structure.[4,5,16] (We define spin frustration here in its more common, general sense of competing exchange interactions of similar magnitude that prevent the preferred spin alignments, rather than the original, more specific sense that competing exchange interactions of the same magnitude lead to a degenerate ground state.) Since the interactions are all antiferromagnetic, they are competing and the precise ground state spin alignment is thus very sensitive to the J_{bw}:J_{bb} ratio, with J_{ww} not being a factor in **8–10** because of its weakness. For example, the typical butterfly complexes **8** and **9** have an $S_T = 3$ ground state spin, the $|S_T, S_A, S_B\rangle = |3, 1, 4\rangle$ state, which results from the dominating J_{bb} interaction aligning the Mn_b spins almost perfectly antiparallel, but not quite (*i.e.* $S_A = 1$ not 0). The J_{bw} interactions are individually weaker than J_{bb}, but there are four of them, and as a result prevent S_A being 0. An intermediate resultant spin is thus obtained in the ground state. In **10**, $J_{bb} \gg J_{wb}$, and the Mn_b spins are now aligned antiparallel, *i.e.* $S_A = 0$, with the weak J_{ww} serving to couple the Mn_w spins antiparallel and giving an overall $S_T = 0$ ground state, the $|S_T, S_A, S_B\rangle = |0, 0, 0\rangle$ state. The ground state of **5–7** can now be satisfactorily rationalized within this description. In fact, it represents the situation at the other extreme compared to **10**, *i.e.* the J_{bb} is now weakened relative to J_{bw} and the two interactions are comparable in magnitude. However, there are four of the latter, and thus J_{bw} now dominates the spin alignments, aligning the spins antiparallel to their neighbors along the outer edges of the $[Mn_4O_2]^{8+}$ butterfly. The J_{bb} interaction is antiferromagnetic but nevertheless completely frustrated, as is J_{ww}, with the two Mn_b spins and the two Mn_w spins both being aligned parallel by the J_{bw} interactions. Thus, the ground state is again $S_T = 0$, as in **10**, but now it is the $|S_T, S_A, S_B\rangle = |0, 4, 4\rangle$ state as depicted in Scheme 2.

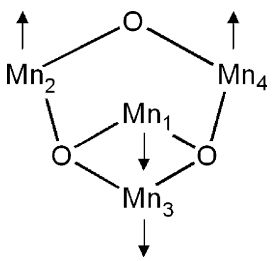

Scheme 2

Conclusions

$SalproH_3$ has proved an effective route to a novel type of tetranuclear Mn complex whose core can be described as a more closed up version of the butterfly-like core that is relatively common. Three isostructural complexes of this new family have been synthesized

and characterized. These complexes also complement and extend the currently rich area of Mn(III) Schiff-base species. Complexes **5–7** extend the type of spin frustration effects observed within the Mn_4 butterfly core, giving an $S_T = 0$ ground state due to total domination of the spin alignments by J_{bw}.

Acknowledgements

This work was supported by the National Science Foundation.

References

1 B. Kok, B. Forbush and M. McGloin, *Photochem. Photobiol.*, 1970, **11**, 457; A. Zouni, H. T. Witt, J. Kern, P. Fromme, N. Krau, W. Saenger and P. Orth, *Nature*, 2001, **409**, 739; N. Kamiya and J. R. Shen, *Proc. Natl. Acad. Sci. USA*, 2003, **100**, 98; K. N. Ferreira, T. M. Iverson, K. Maghlaoui, J. Barber and S. Iwata, *Science*, 2004, **303**, 1831; K. Sauer, J. Yano and V. K. Yachandra, *Photosynth. Res.*, 2005, **85**, 73; V. K. Yachandra, K. Sauer and M. Klein, *Chem. Rev.*, 1996, **96**, 2927; S. Mukhopadhyay, S. K. Mandal, S. Bhaduri and W. H. Armstrong, *Chem. Rev.*, 2004, **104**, 3981.

2 H. Chen, J. W. Faller, R. H. Crabtree and G. W. Brudvig, *J. Am. Chem. Soc.*, 2004, **126**, 7345; S. Mukhopadhyay, H. J. Mok, R. J. Staples and W. H. Armstrong, *J. Am. Chem. Soc.*, 2004, **126**, 9202; S. Wang, K. Folting, W. E. Streib, E. A. Schmitt, J. K. McCusker, D. N. Hendrickson and G. Christou, *Angew. Chem., Int. Ed. Engl.*, 1991, **30**, 305.

3 R. Sessoli, D. Gatteschi, A. Caneschi and M. A. Novak, *Nature*, 1993, **365**, 141; E. M. Chudnovsky, *Science*, 1996, **274**, 938; G. Christou, D. Gatteschi, D. N. Hendrickson and R. Sessoli, *MRS Bull.*, 2000, **25**, 66; A. Caneschi, D. Gatteschi, R. Sessoli, A. L. Barra, L. C. Brunel and M. Guillot, *J. Am. Chem. Soc.*, 1991, **113**, 5873; J. R. Friedman, M. P. Sarachik, J. Tejada and R. Ziolo, *Phys. Rev. Lett.*, 1996, **76**, 3830; A. J. Tasiopoulos, A. Vinslava, W. Wernsdorfer, K. A. Abboud and G. Christou, *Angew. Chem., Int. Ed.*, 2004, **43**, 2117.

4 J. B. Vincent, C. Christmas, H. R. Chang, Q. Li, P. D. W. Boyd, J. C. Huffman, D. N. Hendrickson and G. Christou, *J. Am. Chem. Soc.*, 1989, **111**, 2086.

5 E. Libby, J. K. McCusker, E. A. Schmitt, K. Folting, D. N. Hendrickson and G. Christou, *Inorg. Chem.*, 1991, **30**, 3486.

6 E. K. Brechin, C. Boskovic, W. Wernsdorfer, J. Yoo, A. Yamaguchi, E. C. Sanudo, T. R. Concolino, A. L. Rheingold, H. Ishimoto, D. N. Hendrickson and G. Christou, *J. Am. Chem. Soc.*, 2002, **124**, 9710.

7 K. Bertoncello, G. D. Fallon, K. S. Murray and E. R. T. Tiekink, *Inorg. Chem.*, 1991, **30**, 3562; J. A. Bonadies, M. L. Kirk, M. S. Lah, D. P. Kessissoglou, W. E. Hatfield and V. L. Pecoraro, *Inorg. Chem.*, 1989, **28**, 2037; A. Gelasco and V. L. Pecoraro, *J. Am. Chem. Soc.*, 1993, **115**, 7928; M. Mikuriya, Y. Yamato and T. Tokii, *Bull. Chem. Soc. Jpn.*, 1992, **65**, 1466.

8 Y. Nishida and S. Kida, *J. Chem. Soc., Dalton Trans.*, 1986, **12**, 2633.

9 T. Lis, *Acta. Crystallogr., Sect. B*, 1980, **36**, 2042.

10 J. B. Vincent, H. R. Chang, K. Folting, J. C. Huffman, G. Christou and D. N. Hendrickson, *J. Am. Chem. Soc.*, 1987, **109**, 5703.

11 *SHELXTL6 2000, Bruker-AXS*, Madison, WI, USA.

12 A. R. Schake, J. B. Vincent, Q. Li, P. D. W. Boyd, K. Folting, J. C. Huffman, D. N. Hendrickson and G. Christou, *Inorg. Chem.*, 1989, **28**, 1915.

13 I. D. Brown and D. Altermatt, *Acta Crystallogr., Sect. B*, 1985, **41**, 244; G. J. Palenik, *Inorg. Chem.*, 1997, **36**, 4888; G. J. Palenik, *Inorg. Chem.*, 1997, **36**, 122.

14 K. Kambe, *J. Phys. Soc. Jpn.*, 1950, **5**, 48.

15 J. H. Van Vleck, *The Theory of Electric and Magnetic Susceptibilities*, Oxford Press, London, 1932.

16 G. Aromí, S. Bhaduri, P. Artús, J. C. Huffman, D. N. Hendrickson and G. Christou, *Polyhedron*, 2002, **21**, 1779.

